Protein Synthesis Blockade Prevents Fear Memory Reactivation via inhibition of Engram Synapse Strengthening

Ilgang Hong[1,2,*], Yeonjun Kim[1,2,*], HyunSu Jung[1,2], Chang-Ho Kim[1,3], Jun-Hyeong Cho[4], Bong-Kiun Kaang[1,2,3]

[1]Center for Cognition and Sociality, Institute for Basic Science (IBS), Daejeon, South Korea
[2]Interdisciplinary Program in Neuroscience, Seoul National University, Seoul, South Korea
[3]Department of Biological Sciences, College of Natural Sciences, Seoul National University, Seoul, South Korea
[4]Department of Molecular, Cell and Systems Biology, University of California, Riverside, CA, USA

*These authors contributed equally.
Correspondence to: kaang@ibs.re.kr

Abstract

Memory relies on ensembles of engram cells in the brain. While previous studies have established the existence of these cells, the relationship between cellular and synaptic activity remains unclear. To address this, we applied the dual e-GRASP technique in mice to examine synaptic connectivity between the ventral CA1 and the basal amygdala during memory formation. We found that contextual fear conditioning increased engram-to-engram synapse (engram synapse) density and induced structural potentiation, highlighting their importance in associative memory. Additionally, we investigated the role of protein synthesis in memory formation by inducing retrograde amnesia using anisomycin, a protein synthesis inhibitor. Single anisomycin-injected mice (1xANI) showed impaired natural recall but still displayed fear responses upon optogenetic reactivation of engram cells. In contrast, mice that received four anisomycin injections over six hours (4xANI) showed significantly impaired natural recall and failed to exhibit fear responses upon optogenetic reactivation. This behavioural phenotype was correlated with synaptic changes as 1xANI mice exhibited no significant reduction in engram synapse density but had significantly smaller spine size while 4xANI mice showed both significant reduction in engram synapse density and spine size. Our result indicate that protein synthesis inhibition significantly changes engram synapse density and spine size which correlatively affect fear memory natural recall and artificial reactivation.

Introduction

The concept of the engram refers to the physical trace of a memory, which operates across multiple scales[1]. This synaptic engram has been studied in various behavioural paradigms—including contextual fear conditioning, auditory fear conditioning, and motor learning—as well as across different memory stages, such as consolidation, extinction, and remote recall[2–5]. However, whether this hypothesis extends beyond the CA3-CA1 circuit in fear learning

remains unclear. In this study, we explore the engram synapse hypothesis within the ventral CA1 (vCA1) – basal amygdala (BA) circuit during associative fear learning.

The vCA1 is known to play a critical role in aversive learning, with growing evidence suggesting that engram neurons within this region encode information essential for forming lasting associations such as linking a specific environment to an aversive outcome. Conversely, the amygdala is widely recognised for its role in processing emotions, especially fear-related responses. Within this framework, activated vCA1 neurons are thought to convey contextual representations to the BA. Although the anatomical and functional connectivity between vCA1 and BA has been demonstrated in both *ex vivo* and *in vivo* studies, direct visualization of this connection at the synaptic level remains largely unexplored.

Protein synthesis is known to be critical in long-lasting forms of synaptic plasticity. Applying a protein synthesis inhibitor (PSI) such as cycloheximide or anisomycin in brain slices prior to tetanisation has been shown to reduce the amplitude of field excitatory postsynaptic potentials and impair synaptic transmission during the late phase of long-term potentiation[6–8]. Consequently, inhibiting protein synthesis during acquisition blocks natural recall[9]. As anticipated, the disruption of memory consolidation is accompanied by the loss of enhanced synaptic strength in engram cells[9,10].

Protein synthesis is essential for natural memory recall, but its role in memory storage and artificial recall remains debated. A single anisomycin injection after memory acquisition impairs natural recall, yet optogenetic reactivation of DG engram cells can still induce memory retrieval[9]. However, when anisomycin is administered alongside tat-Beclin, an autophagy-inducing drug, both natural and artificial recall are disrupted[11]. This raises the question of

84 whether memory storage and artificial recall are critically affected by the magnitude of protein
85 synthesis blockade. Additionally, the synaptic changes associated with protein synthesis
86 blockade remain unclear. Here, we demonstrate that in the vCA1-BA circuit, the impairment
87 of both natural recall and optogenetic reactivation depends on the degree of protein synthesis
88 inhibition, which correlates with reductions in engram synapse density and spine size.
89

90 ## Results

91 **Validation of vCA1-BA circuit during contextual fear memory**

92 The inner and the outer layers of vCA1 projecting to the BA are known to play distinct roles
93 in fear memory, but also in anxiogenic and anxiolytic behaviour[12–14]. To determine which layer
94 projects to the BA, retrograde viral tracing was performed by injecting retrogradely transducing
95 CAV-Cre into the BA of double-floxed tdTomato mice. Retrograde tracing confirmed that BA-
96 projecting vCA1 neurones mainly reside in the outer layer (Fig. S1).
97

98 Next, to see whether each neurone can store fear memory as an engram cell, the reactivation
99 ratio between acquisition- and retrieval-activated cells was observed. Acquisition-activated
100 neurones were labelled using fos promoter driven tet-on system and recall-activated neurones
101 were labelled using fos immunohistochemistry (Fig. S2 A, B). A significant increase in
102 colocalisation ratio was observed in the contextual fear conditioning (CFC) group compared to
103 the naïve group in both vCA1 and BA (Fig. S2 C-E).
104

105 **Increased synaptic density and spine size between vCA1 and BA engram cells during**
106 **memory formation**

107 Next, correlation between associative memory formation and synaptic connectivity between
108 engram cells was assessed. Dual enhanced green fluorescent protein reconstitution across

synaptic partners (dual-eGRASP) enables specific labelling of activated dendrites and synapses. Dual-eGRASP utilises split protein reconstitution in the synaptic cleft to label synapses. Using two colours of split protein and fluorescence expression, all connection types between engrams (E) and non-engrams (N) can be fluorescently labelled (Fig. 1A-C, S3A). Using this dual-eGRASP technique, synaptic strengthening was quantified in the vCA1-BA circuit after CFC (Fig. 1B, S3B). No significant difference in synaptic density was observed between N-N and N-E across all experimental groups while significantly higher density of E-E synapses was observed in the CFC group compared to the E-N synapses (Fig. 1D). This suggests recruitment of synapses between engram neurones during acquisition of associative memory. Subsequently, morphological changes were investigated to confirm structural plasticity in the spines during associative memory formation. Morphological analysis revealed a significant increase in spine head diameter, spine head volume, and spine volume of E-E synapses in the CFC group compared to N-E synapses (Fig. 1E). The context only group exhibited no significant differences in spine head size of E-E synapses. We conclude that fear conditioning induced structural plasticity specifically in E-E synapses. No significant difference was found in any of the four metrics of structural plasticity between N-N and N-E synapse in the three behavioural groups (Fig. S3F). Consequently, these results indicate that engram synapses undergo structural plasticity during associative fear learning in the vCA1-BA circuit.

De novo **protein quantification using NCAA labelling**

A key aspect of memory consolidation theory suggests that *de novo* protein synthesis is essential for synaptic plasticity[15,16]. The use of PSIs has been crucial in advancing this theory, as numerous studies have demonstrated that administering PSIs during memory acquisition impairs natural recall in mice[9]. Therefore, as an indirect method to inhibit synaptic changes observed in Fig 1, we established PSI treatment behavioral conditions with greater specificity.

First, to establish experimental conditions for extensive protein synthesis inhibition, noncanonical amino acids (NCAA) labelling was performed as mice were injected with PSI. Given that the reported time window for memory consolidation extends up to 6 hours after the event[17], initial approach aimed to extend the duration of the PSI treatment[18–20]. It has been previously reported using an electrophysiological approach that four consecutive injections of anisomycin weaken E-E synaptic strengthening[21]. Therefore, mice received four consecutive anisomycin injections (4xANI), or a single anisomycin injection followed by three consecutive saline injections (1xANI), or 4 consecutive saline injections (SAL). Immediately after the CFC, mice were intraperitoneally injected with L-methionine analog L-azidohomoalanine (AHA) and brains were snap frozen 16 hours after CFC (Fig. 2A). Quantification of NCAA labelled proteins by western blotting showed that 4xANI mice displayed protein intensity comparable to that of AHA^- mice (Fig. 2B, C). These results suggest that 4xANI injections effectively suppresses protein synthesis.

Multiple injections and cocktail of drugs induce retrograde amnesia more effectively

Building on NCAA studies, robust protein synthesis inhibition conditions were applied *in vivo*. For multiple injections, four consecutive injections of saline or anisomycin were delivered (Fig. 2A, D). In another experimental condition, a stronger inhibition was achieved with a single injection by using cycloheximide along with anisomycin to inhibit two different ribosomal sites (Fig. S5). In line with the previous study, a single injection of anisomycin decreased natural recall of fear memory[9], while multiple injections of anisomycin and the cocktail group (CKT) exhibited significantly lower freezing levels compared to the single injected group (Fig. 2E, 2H, S5A-B). Therefore, these data confirm that extensive protein synthesis inhibition by

158 multiple injections of anisomycin or a cocktail of protein synthesis inhibitors significantly
159 impairs natural recall of fear memory.
160
161 To test whether the memory impairment by injection of PSI leads to impaired engram
162 reactivation, Arc-CreERT2 crossed with floxed tdTomato mice were fear conditioned followed
163 by 4-OHT and a series of PSI injections (Fig. 2D). Immunohistochemistry analysis showed no
164 significant difference in the ratio of tdTomato^{+} or Fos^{+} neurones in all three groups (Fig. S4).
165 However, the reactivation ratio between activated neurones during the conditioning and
166 memory recall was significantly lower in the 4xANI group in both vCA1 and BA (Fig. 2I, J).
167 Significant differences in reactivation ratio between groups were replicated using Arc-
168 CreERT2 mice expressing CaMKII-DIO-tdTomato (Fig. 2F, G). Moreover, the single injection
169 of the cocktail significantly reduced the reactivation ratio in the BA compared to treatment
170 with anisomycin alone (Fig. S5). Taken together, these data suggest that multiple injections of
171 anisomycin significantly disrupt the reactivation of engram cells and impair memory recall.
172
173 We next examined whether amnesic memory can be recalled using optogenetics. To reactivate
174 neurones specifically activated during the CFC under different PSI treatments, EF1a-DIO-
175 ChR2-eYFP was bilaterally expressed in the vCA1 of Arc-CreERT2 mice (Fig. 3B, S6A). To
176 reach sufficient virus expression in axon terminals in the BA, mice were tested five days after
177 the CFC (Fig. S6B, C). Restoration of memory from amnesia has been observed by directly
178 stimulating anisomycin-treated DG engram cells with light; this preferential, protein synthesis-
179 independent functional engram connectivity was observed even eight days after the initial
180 training[22]. All groups of mice reported here showed robust freezing acquisition (Fig. 3A). Five
181 days after training, mice were introduced to a novel environment for blue light stimulation. In
182 line with prior research, neither group displayed freezing behaviour when the blue light was

183 off, but SAL groups and 1xANI groups exhibited a significant increase in freezing behaviour
184 when the blue light was on (Fig. 3C-D, S7C-D). Notably, in the CKT and 4xANI group, mice
185 did not display any freezing level during the light on and off sessions (Fig. 3E, Fig. S7E). To
186 assess the conditioned response to recall cues, mice were once more evaluated in the fear-
187 conditioned chamber 24 hours after the optical stimulation. Consistent with our previous data,
188 SAL mice showed robust freezing while 4xANI showed minimal freezing behaviour (Fig. 3B).
189
190 The saline group displayed robust freezing behaviour, whereas the anisomycin group with
191 single injection resulted in significantly reduced freezing behaviour during cued recall (Fig.
192 S7B). The 4xANI and CKT groups exhibited a freezing level similar to naïve mice. These data
193 indicate that the connectivity of vCA1 engram cells to the downstream BA is enhanced during
194 memory acquisition only if the protein synthesis blockade is not extensive, while an extensive
195 blockade inhibits synaptic strengthening between the regions, thus impairing memory.
196
197 Collectively, these data provide evidence supporting the critical role of engram synapses in
198 associative memory by indirectly modulating engram synapse potentiation by multiple PSI
199 injections.
200
201 To investigate the synaptic changes associated with memory under extensive protein synthesis
202 blockade, we applied the dual-eGRASP technique (Fig. 1A). Mice underwent CFC followed
203 by serial injections of either anisomycin or saline (Fig. 4A). Consistent with our previous
204 findings, the group that received four injections of anisomycin (4xANI) exhibited significantly
205 impaired fear memory retrieval compared to the SAL group (Figs. 3B and 4B). Dual-eGRASP
206 analysis revealed an increased density of E-E synapses across all behavioural groups, while no
207 significant differences were observed in N-E synapse density (Figs. 1D and 4C). However, a

208 notable reduction in E-E synapse density was observed in the 4xANI group compared to the
209 1xANI, with no significant difference between the SAL and 1xANI groups (Fig. 4C). This
210 reduction in E-E synapse density may explain the failure of optogenetic reactivation observed
211 in the 4xANI group (Fig. 3E). Additionally, spine morphology analysis revealed increases in
212 spine head diameter, spine head volume, and overall spine volume in the E-E synapses of the
213 SAL group (Figs. 1E and 4D, E). Interestingly, these metrics showed no significant changes in
214 the 1xANI or 4xANI groups, with spine dimensions in the 1xANI group being significantly
215 smaller than those in the SAL group. These findings suggest that the reduction in spine
216 dimensions correlates with impaired natural memory recall observed in the 1xANI group (Fig.
217 3D).
218

219 **Discussion**

220 It has been challenging to determine whether memory formation strengthens the synapses
221 between engram cells in interconnected brain regions[23]. This challenge stems from the
222 difficulty in distinguishing presynaptic regions formed by engram cells from those formed by
223 non-engram cells. The modification of the GRASP technique has provided the solution
224 enabling the visualisation and analysis of spine density and morphology. Additionally, by
225 positioning the colour-determining domain in the presynaptic neurone (cyan/yellow pre-
226 eGRASP) and the common domain in the postsynaptic neurone (post-eGRASP), we have
227 successfully visualised two synaptic populations originating from two distinct presynaptic
228 neuronal populations, both projecting to a single postsynaptic neurone[2].
229

230 Using the dual-eGRASP technique we investigate the hypothesis that contextual fear learning
231 is associated with the enhancement of synapses between engram cells, the so-called synaptic
232 engram hypothesis. Engram synapses have been shown to be critical in memory acquisition

233 and extinction where changes in engram synapse density and spine head size were observed[2,3].
234 Our results showed similar lines of data, where increased synapse density, spine head size,
235 spine volume, and spine head volume were observed specifically in E-E synapses of vCA1-BA
236 circuit (Fig. 1D, E). Therefore, these data suggest that the engram synapse hypothesis can also
237 be applied to the vCA1-BA circuit during associative fear learning.
238
239 Along with the CFC group, the context only group also exhibited an increase in E-E synaptic
240 density (Fig. 1D). This data is consistent with our previous findings within the CA3-CA1
241 pathway, where the context only group demonstrated significant synaptic changes[2]. This
242 increase in synaptic density may be attributed to Hebbian plasticity between vCA1 engram
243 neurones and BA neurones activated by emotions other than fear, such as anxiety, generated
244 during exposure to the novel context[24] as BA is also known to mediate anxiogenic behaviour[14].
245 Unlike synaptic activity of the vCA1 region drives the increase in synaptic density, although it
246 is not sufficiently pronounced to increase spine size.
247
248 Moreover, to validate the hypothesis that modification of E-E synaptic connectivity is
249 necessary for memory acquisition, we administered a PSI to induce retrograde amnesia. In this
250 study, we set the optimal conditions for inducing extensive retrograde amnesia that cannot be
251 artificially recalled (Fig. 3E, S7E). By extending the time window of protein synthesis
252 inhibition or simultaneously targeting two ribosomal sites, we show that these experimental
253 conditions induce a more pronounced effectiveness in impairing memory recall.
254
255 It has been reported that a memory that is impaired by inhibiting synaptic potentiation using
256 PSI can later be artificially reactivated[9]. Another study has demonstrated that inhibiting protein
257 synthesis, coupled with the induction of autophagy, results in irretrievable memory[11]. To assess

258 whether varying degrees of protein synthesis inhibition produce different behavioural
259 outcomes, we tested multiple groups to identify the optimal condition for inducing memory
260 impairment. This approach led to the discovery that when mice undergo an extensive inhibition
261 of protein synthesis, optogenetic reactivation of engram cells can no longer induce memory
262 recall. Multiple injections of anisomycin showed no significant changes to the number of
263 engram cells (Fig. S4D). Also, E-E synapses showed increased density and enlarged structural
264 morphology during associative fear learning (Fig. 1D, E). Therefore, we propose that the failure
265 of optogenetic reactivation in mice subjected to multiple anisomycin injections is attributed to
266 a reduction in E-E synaptic density caused by extensive protein synthesis inhibition (Fig. 4B).
267 On the other hand, we suggest that the impaired natural recall observed in both 1xANI and
268 4xANI groups is driven by the lack of engram synapse enlargement (Fig.4C). Numerous studies
269 have provided evidence that neither single nor multiple injections of anisomycin are sufficient
270 to block synaptic plasticity to a level comparable to the naïve group[9,21]. Although the
271 AMPAR/NMDAR ratio was lower, EPSC frequency remained elevated, suggesting that
272 synaptic strength weakened while E-E synaptic connections increased[21]. We can conclude that
273 our experimental conditions were sufficient to impair memory recall in both natural and
274 optogenetic reactivation contexts (Fig. 3, 4). However, the residual freezing behaviour and the
275 observed increase in engram synapse density needs further investigation which may be
276 regulated by protein synthesis independent mechanisms such as remodelling of actin skeleton.
277
278 Limitations of the current study arise from the fact that anisomycin affects protein synthesis in
279 a non-discriminative way. Anisomycin was treated by intraperitoneal injection, thereby
280 affecting the whole mouse body. To rule out the possibility that protein synthesis blockade
281 from other regions has contributed to the failure of memory storage, future studies should block

282 protein synthesis in a brain region-specific and engram-specific manner possibly through the
283 use of genetically encodable PSI[25].
284

285 # References

286 1. Josselyn, S. A., Köhler, S. & Frankland, P. W. Finding the engram. *Nat. Rev.*
287 *Neurosci. 2015 169* **16**, 521–534 (2015).
288 2. Choi, J. H. *et al.* Interregional synaptic maps among engram cells underlie memory
289 formation. *Science (80-.).* **360**, 430–435 (2018).
290 3. Choi, D. Il *et al.* Synaptic correlates of associative fear memory in the lateral
291 amygdala. *Neuron* **109**, 2717-2726.e3 (2021).
292 4. Lee, C. *et al.* Hippocampal engram networks for fear memory recruit new synapses
293 and modify pre-existing synapses in vivo. *Curr. Biol.* **33**, 507-516.e3 (2023).
294 5. Kim, Y., Hong, I. & Kaang, B. K. Synaptic correlates of the corticocortical circuit in
295 motor learning. *Philos. Trans. R. Soc. Lond. B. Biol. Sci.* **379**, (2024).
296 6. Schafe, G. E. *et al.* Activation of ERK/MAP kinase in the amygdala is required for
297 memory consolidation of pavlovian fear conditioning. *J. Neurosci.* **20**, 8177–8187
298 (2000).
299 7. Schafe, G. E. & LeDoux, J. E. Memory consolidation of auditory pavlovian fear
300 conditioning requires protein synthesis and protein kinase A in the amygdala. *J.*
301 *Neurosci.* **20**, (2000).
302 8. Fonseca, R., Vabulas, R. M., Hartl, F. U., Bonhoeffer, T. & Nägerl, U. V. A balance of
303 protein synthesis and proteasome-dependent degradation determines the maintenance
304 of LTP. *Neuron* **52**, 239–245 (2006).
305 9. Ryan, T. J., Roy, D. S., Pignatelli, M., Arons, A. & Tonegawa, S. Engram cells retain
306 memory under retrograde amnesia. *Science (80-.).* **348**, 1007–1013 (2015).

307 10. Roy, D. S. *et al.* Memory retrieval by activating engram cells in mouse models of early
308 Alzheimer's disease. *Nature* **531**, 508–512 (2016).
309 11. Abdou, K. *et al.* Synapse-specific representation of the identity of overlapping memory
310 engrams. *Science (80-.).* **360**, 1227–1231 (2018).
311 12. Gergues, M. M. *et al.* Circuit and molecular architecture of a ventral hippocampal
312 network. *Nat. Neurosci.* **23**, 1444–1452 (2020).
313 13. Jimenez, J. C. *et al.* Contextual fear memory retrieval by correlated ensembles of
314 ventral CA1 neurons. *Nat. Commun. 2020 111* **11**, 1–11 (2020).
315 14. Pi, G. *et al.* Posterior basolateral amygdala to ventral hippocampal CA1 drives
316 approach behaviour to exert an anxiolytic effect. *Nat. Commun.* **11**, (2020).
317 15. Kandel, E. R. The molecular biology of memory storage: a dialogue between genes
318 and synapses. *Science* **294**, 1030–1038 (2001).
319 16. Costa-Mattioli, M., Sossin, W. S., Klann, E. & Sonenberg, N. Translational control of
320 long-lasting synaptic plasticity and memory. *Neuron* **61**, 10–26 (2009).
321 17. Casagrande, M. A. *et al.* Synaptic consolidation as a temporally variable process:
322 Uncovering the parameters modulating its time-course. *Neurobiol. Learn. Mem.* **150**,
323 42–47 (2018).
324 18. Squire, L. R., Kuczenski, R. & Barondes, S. H. Tyrosine hydroxylase inhibition by
325 cycloheximide and anisomycin is not responsible for their amnesic effect. *Brain Res.*
326 **82**, 241–248 (1974).
327 19. Flood, J. F., Bennett, E. L., Orme, A. E., Rosenzweig, M. R. & Jarvik, M. E. Memory:
328 Modification of anisomycin-induced amnesia by stimulants and depressants. *Science*
329 *(80-.).* **199**, 324–326 (1978).
330 20. Freeman, F. M., Rose, S. P. R. & Scholey, A. B. Two Time Windows of Anisomycin-
331 Induced Amnesia for Passive Avoidance Training in the Day-Old Chick. *Neurobiol.*

332 *Learn. Mem.* **63**, 291–295 (1995).
333 21. Kim, W. Bin & Cho, J. H. Encoding of contextual fear memory in hippocampal–
334 amygdala circuit. *Nat. Commun.* **11**, 1–22 (2020).
335 22. Roy, D. S., Muralidhar, S., Smith, L. M. & Tonegawa, S. Silent memory engrams as
336 the basis for retrograde amnesia. *Proc. Natl. Acad. Sci. U. S. A.* **114**, E9972–E9979
337 (2017).
338 23. Hebb, D. 0. The Organization of Behavior A NEUROPSYCHOLOGICAL THEORY.
339 (1949).
340 24. Tye, K. M. *et al.* Amygdala circuitry mediating reversible and bidirectional control of
341 anxiety. *Nature* **471**, 358–362 (2011).
342 25. Heumüller, M., Glock, C., Rangaraju, V., Biever, A. & Schuman, E. M. A genetically
343 encodable cell-type-specific protein synthesis inhibitor. *Nat. Methods 2019 168* **16**,
344 699–702 (2019).
345 26. Fripont, S., Marneffe, C., Marino, M., Rincon, M. Y. & Holt, M. G. Production,
346 purification, and quality control for adeno-associated virusbased vectors. *J. Vis. Exp.*
347 **2019**, e58960 (2019).
348

349

350 # Materials and methods

351 **Animals**

352 All experiments were conducted in accordance with the regulations and guidelines of the
353 Institutional Animal Care and Use Committees (IACUC) of Seoul National University.
354 Investigators were not blinded to the genotypes of the mice.

355

356 Wild-type C57BL/6N mice were used for dual-eGRASP experiments, while wild-type
357 C57BL/6J mice were used for BONCAT. Heterozygous Arc-CreERT2 (Jackson Laboratory
358 Stock # 022357) mice, obtained by crossing wild-type C57BL6/J and Arc-CreERT2 (+/−) mice,
359 were utilised to label engram neurones and for optogenetic experiments. Heterozygous Arc-
360 CreERT2; Ai14 mice, obtained by crossing Ai14 (Jackson Laboratory Stock # 007914) and
361 Arc-CreERT2 (+/−) mice, were used to label engram neurones in the experiments.
362
363 Mice were housed in standard laboratory cages with disposable bedding on a standard light
364 cycle (09h-21h). Mice had access to food and water *ad libitum* and were socially housed in
365 numbers of three to five littermates until surgery. Behavioural experiments were performed
366 during the light cycle. Male and/or female mice were utilised in the experiments with details
367 provided in the figures or figure legends
368
369 **AAV production**
370 Adeno-associated virus serotype 1/2 (AAV1/2; AAV particle containing both serotype 1 and 2
371 capsids) was used for injection, as previously described[2].
372
373 The procedure for packaging plasmids into adeno-associated virus serotype 9 (AAV9) involved
374 the following steps: Plasmids containing the construct of interest flanked by AAV2 ITR, pAd-
375 ΔF6, and pRep/Cap9 were co-transfected into the AAVpro 293T Cell Line (TAKARA, cat#
376 632273). The transfected cells were then incubated in DMEM with 10% v/v FBS for five days
377 in a 150 mm culture dish. On the day of harvest, culture medium was collected and the
378 remaining cells were lysed to extract any virus they contained. After centrifugation at 13,490
379 g for 60 minutes at 4°C, the supernatants were carefully loaded into ultracentrifugation tubes
380 filled with iodixanol gradient solutions.

381

382 AAV was purified from the cell lysate using iodixanol density-gradient ultracentrifugation as
383 previously described[26]. 40% iodixanol solutions were withdrawn using 5 mL syringes and
384 further concentrated using Amicon Ultra 100-kDa MWCO ultrafiltration centrifugal devices
385 (Merck, cat# UFC910024).

386

387 **Virus-mediated gene expression**

388 For cFos labelling experiments, the virus comprised AAV1/2-Fos-rtTA mixed with AAV1/2-
389 TRE-mCherryNuc. Virus was bidirectionally injected into both vCA1 (500 nl; AP: -3.1 mm,
390 ML: ±3.4 mm DV: -3.8 mm) and BA (500 nl; AP: -1.5 mm ML: ±3.0 mm, DV: -4.9 mm).

391

392 The AAV9-CaMKII-ChR2-EYFP and AAV9-CaMKII-EYFP was packaged as described. The
393 plasmids were acquired from Addgene and were serotyped with AAV9 coat proteins and
394 packaged as described. AAV9- EF1α-DIO-ChR2-EYFP was acquired from Institute for Basic
395 Science Recombinant Virus Packaging Facility.

396

397 **Stereotactic surgery procedure**

398 Mice were anaesthetised by intraperitoneal injection of 25 $mg \cdot kg^{-1}$ ketamine /xylazine and
399 positioned on a stereotaxic apparatus (Stoelting Co.). Ophthalmic ointment was applied to the
400 eyes as a preventive measure against dryness. Bilateral craniotomies were performed using a
401 0.5 mm diameter drill and the viruses were injected using a micro-needle attached to a 10 mL
402 Hamilton micro syringe (Hamilton; cat# 701LT). A syringe driver (WPI, cat# SP3101-PLUS)
403 was used to maintain the speed of the injection at 0.125 $ul \cdot min^{-1}$. The needle was slowly
404 lowered to the target site and remained for 2 minutes before beginning the injection. After
405 injection, the needle stayed for 10 minutes before it was slowly withdrawn. The incision was

406 sutured, and mice were allowed to recover for 2 weeks before the start of behavioural
407 experiment.
408
409 For the optogenetic experiment, a custom implant containing two optic fibres (Newdoon; 0.37
410 NA 1.25 mm core diameter) was lowered above the injection site at the following coordinate
411 relative to bregma (mm): AP: -1.5 ML: ±3.0 DV: -4.0 for BA. A jewellery screw was screwed
412 into the skull near the bregma. Mice were allowed to recover for at least 2 weeks before
413 behavioural experiments.
414
415 **Contextual fear conditioning**
416 Two weeks following AAV injection, all mice underwent a conditioning procedure. Prior to
417 conditioning, each mouse was housed individually for eight days and was subjected to daily
418 handling sessions lasting five minutes for seven consecutive days. Mice were randomly
419 assigned to either the CFC group or the context only control group. Mice were transferred from
420 the vivarium to a holding room adjacent to the testing area at least 30 minutes prior to the start
421 of the experiment. Furthermore, each mouse was transported individually to the conditioning
422 room.
423
424 The conditioning chamber measuring 7”W × 7”D × 12”H (Coulbourn Instruments; model H10-
425 11M-TC)was used. The chamber featured two aluminium side walls and a ceiling with an
426 acrylic door. It was situated within a larger sound-attenuating enclosure. Throughout the
427 experimental procedures, a white overhead light continuously illuminated the conditioning
428 chamber. The chamber itself was equipped with a straight stainless-steel rod floor which was
429 cleaned using a 70% ethanol solution and distilled water between each use.
430

431 Two hours prior to the conditioning procedure, an intraperitoneal injection of 250 μL of a 5
432 $mg \cdot ml^{-1}$ Doxycycline solution dissolved in saline was administered. For contextual fear
433 conditioning, mice were exposed to the context for 180 seconds, after which five-foot shocks
434 were delivered where each foot shock lasted 2 seconds with an interval of 2 minutes. Following
435 the conditioning session, mice were returned to their respective home cages. During the
436 retrieval test, the percentage of time spent freezing was calculated and averaged across the
437 entire 3-minute retrieval session.
438
439 **Optogenetics**
440 For the single injection groups, mice were either injected with saline, anisomycin, or
441 anisomycin + cycloheximide right after conditioning. For the multiple injection groups, mice
442 were first injected with saline or anisomycin, followed by three injections with saline or
443 anisomycin at 2 hours of intervals. 4-OHT was injected intraperitoneally for 50 $mg \cdot kg^{-1}$10
444 minutes after the first injection. For the immunohistochemistry, mice were retrieved two days
445 after the conditioning and perfused 90 minutes after retrieval. For optogenetics, mice were
446 habituated to optical cables for at least 30 minutes before the experiment. From 30 to 60
447 minutes of habituation, mice were placed in the acrylic chamber. Mice were allowed to freely
448 move within the acrylic chamber and freezing behaviour was recorded for 8 minutes, with 2
449 minutes of two consecutive lights 'off' and 'on' sessions.
450
451 **Immunohistochemistry**
452 90 minutes after retrieval, mice were deeply anesthetised using ketamine/xylazine (15 $mg \cdot kg^{-}$
453 ^{1}) followed by transcranial perfusion with 15 ml of PBS and 15 ml of 4% PFA. Brains were
454 removed, post-fixed overnight at 4°C in 4% PFA and dehydrated in a 30% sucrose solution in
455 PBS at 4°C for two days. The brain was rinsed with PBS and subsequently frozen at -80°C for

456 a minimum of one hour. Coronal sectioning was performed using a cryostat (Leica) with a
457 thickness of 30 μm. The sections were rinsed with 1 mL of PBS for 5 minutes each time at
458 room temperature (RT), 120 rpm. Then 500 μL of a blocking solution (5% normal goat serum,
459 0.3% triton X-100 in PBS) was applied to each sample for 1hr RT, 80 rpm. The primary c-Fos
460 antibody (SySy, cat# 226 003) was applied at a concentration of 1:1000 for 24 hours on a
461 shaker at 4 °C. Sections were washed three times with PBS for 5 minutes each time at room
462 temperature (RT), 120 rpm. A secondary antibody (Alexa-488; 1:500) was applied at a
463 concentration of 1:500 for 2 hours at 80 rpm. Finally, sections were washed with 1 mL of PBS
464 three times for 5 minutes each time at 120 rpm, RT. The second washing step included DAPI
465 staining at a concentration of 1:1000 for 5 minutes at 80 rpm, RT. Cell counting was manually
466 performed using Imaris (Bitplane) by an experimenter who was blinded to the conditions.
467
468 **Confocal imaging**
469 10-15 z-stacks per animal were taken for the immunohistochemistry analysis. Around
470 50-100 z-stacks were taken for the dual-eGRASP density analysis, while 30-50 z-stacks of the
471 image were used to analyse synaptic morphology. All samples were imaged using Leica SP8
472 confocal microscope with 63x objective with distilled water immersion and 10x objective lens
473 was used for the immunohistochemistry. Images were taken within −2.9 to −3.8 mm bregma,
474 spanning a range of ventral CA1 and -1.3 to 1.8 mm bregma for the BA.
475
476 Each dendrite expressing mScarlet-I or iRFP670 was identified and manually labelled as a
477 filament using a filament tracer in IMARIS. To eliminate bias, other fluorescent signals were
478 concealed. Cyan or yellow eGRASP signals were automatically detected and marked as cyan
479 or yellow spheres. An overlap between cyan and yellow eGRASP signals was considered a
480 yellow signal as it indicated that the presynaptic neurone of the synapse was c-fos+ during

memory formation. Dendrites lacking cyan or yellow eGRASP signals were excluded from further detailed analysis.

Spines on the designated mScarlet-I+ and iRFP670+ dendrites were manually reconstructed, and their diameter and volume were automatically detected. Each spine was categorised as either an activated spine or a non-activated spine based on the presence of a yellow or cyan eGRASP signal, determined through manual inspection. Measurements of spine head diameter, spine head volume, and spine length were performed using Imaris Filament Tracer. Importantly, the examiner conducting the spine 3D model reconstructions was kept blind to any eGRASP signals to prevent bias. Normalisation of the raw data was performed on a per-image basis to measure synaptic density and on a per-dendrite basis for morphology analysis. For the iRFP dendrite (for density analysis) or cyan-only spine morphology, the raw values were averaged, and then the raw values of each cyan-only spine and yellow spine were divided by this average. The resulting normalised values were utilised for subsequent statistical analysis.

Statistical analysis

Data were analysed using a non-parametric Mann-Whitney U-test. Data analysis was performed on Prism (GraphPad Software). The α value was set at 0.05 for all analyses. All data are presented as mean ± SEM.

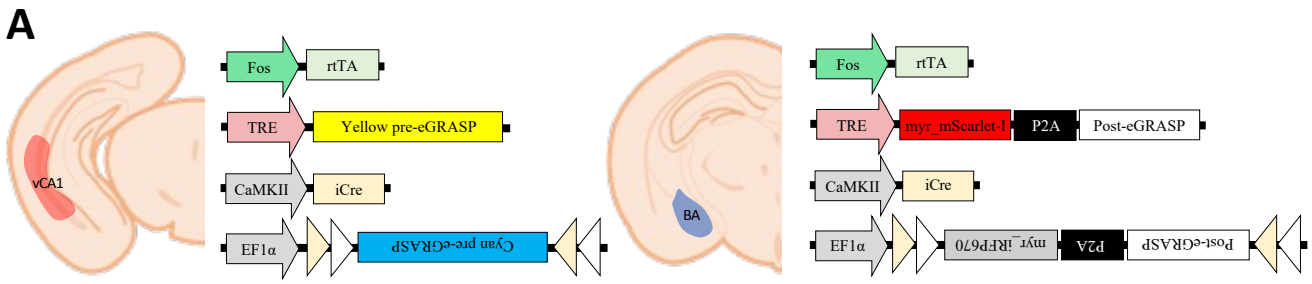
A
vCA1
Fos
rtTA
TRE
Yellow pre-eGRASP
CaMKII
iCre
EF1α
Cyan pre-eGRASP
BA
Fos
rtTA
TRE
myr_mScarlet-I
P2A
Post-eGRASP
CaMKII
iCre
EF1α
myr_iRFP670
P2A
Post-eGRASP

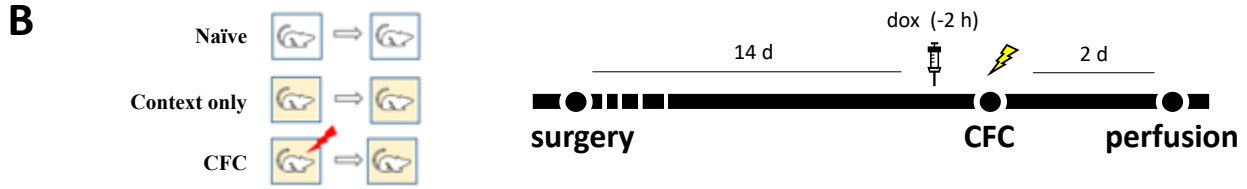
B
Naïve
Context only
CFC
dox (-2 h)
14 d
2 d
surgery
CFC
perfusion

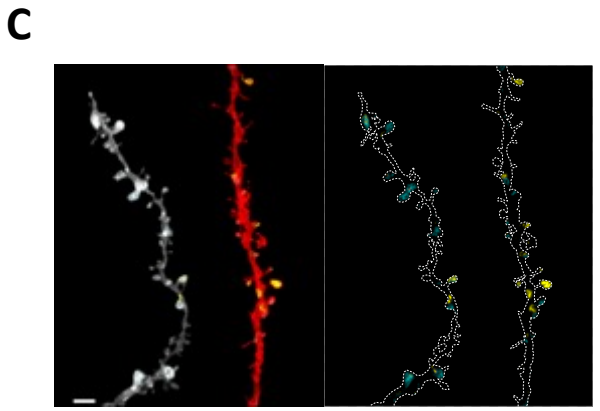
C

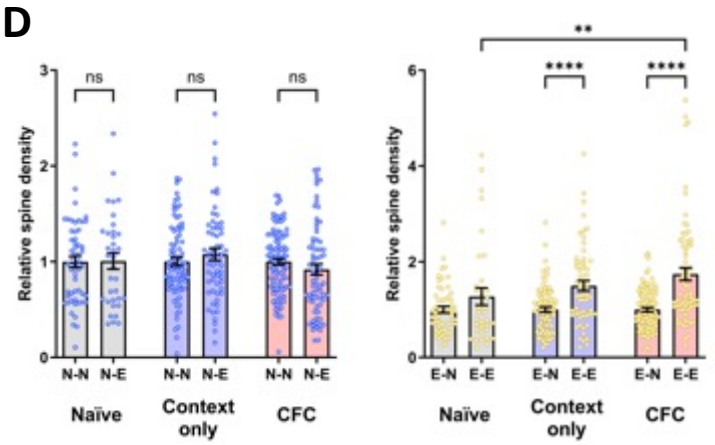
D
Relative spine density
ns
ns
ns
N-N N-E N-N N-E N-N N-E
Naïve
Context only
CFC
**
****
****
E-N E-E E-N E-E E-N E-E
Naïve
Context only
CFC

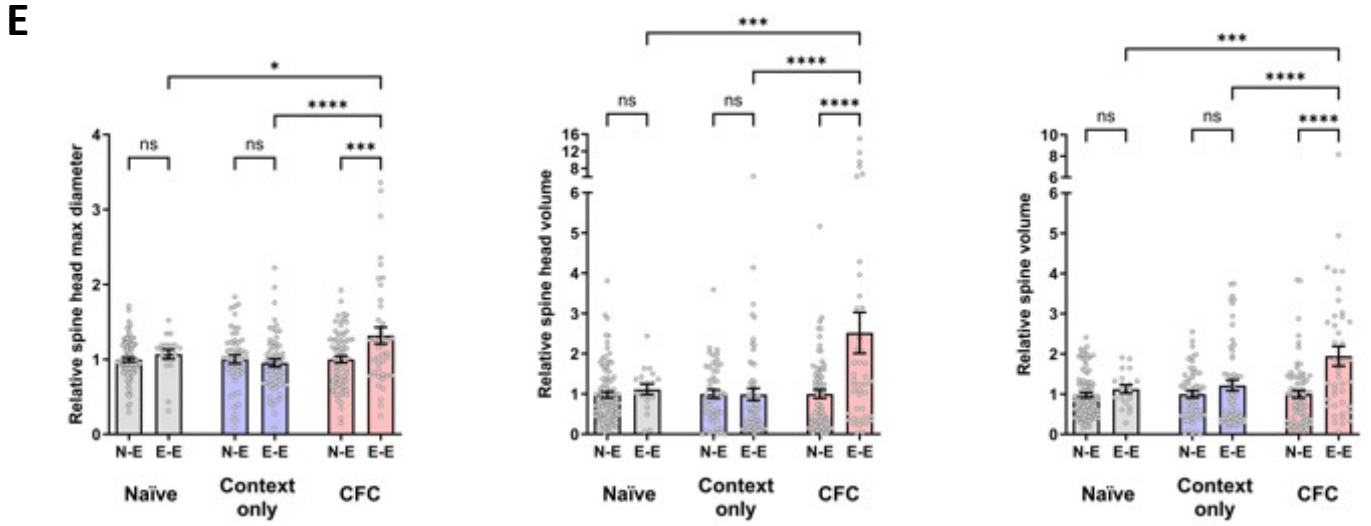
E
Relative spine head max diameter
*
****
ns
ns
***
N-E E-E N-E E-E N-E E-E
Naïve
Context only
CFC
Relative spine head volume
***
****
ns
ns
****
N-E E-E N-E E-E N-E E-E
Naïve
Context only
CFC
Relative spine volume
***
****
ns
ns
****
N-E E-E N-E E-E N-E E-E
Naïve
Context only
CFC

Figure 1. Synaptic density between the vCA1-BA pathway

(**A**) Illustration of virus injection sites. Injection in each site was performed with a cocktail of all the viruses shown for each site.

(**B**) Schematic of the experimental protocol.

(**C**) Illustrative image depicts both engram (red) and nonengram (gray) dendrites with dual-eGRASP labelling in the BA. Cyan signals represent random vCA1 inputs while yellow signals indicate vCA1 engram inputs. Scale bar : 3 μm

(**D**) Normalised cyan/yellow eGRASP per dendritic length. The densities of cyan-only or yellow puncta on mScarlet-I^{+} dendrites are normalised to the corresponding cyan-only or yellow puncta on iRFP670^{+} dendrites from the same images to exclude the effect of different number of vCA1 cells expressing each presynaptic component. Each data point represents a dendrite. Naïve group, n = 45 for BA non engram dendrites, n = 27 for BA engram dendrites; Context only group, n = 106 for BA non engram dendrites; n = 66 for BA engram dendrites; CFC group, n = 73 for BA non engram dendrites; n = 62 for BA engram dendrites. Two-way ANOVA followed by Tukey's multiple comparison test. **P = 0.0063; ****P < 0.0001. Data are presented as mean ± SEM.

(**E**) Normalised spine head diameters, spine head volume and spine volume of dendrites from BA engram cells. Naïve group N-E, n = 111; E-E, n = 32; Context only group N-E, n = 107; E-E, n = 75; CFC group N-E, n = 71; E-E, n = 37. Two-way ANOVA followed by Tukey's multiple comparison test. spine head diameter *P = 0.0315; ***P = 0.0001, spine head volume ***P = 0.0004; ****P < 0.0001, spine volume ***P = 0.0001; ****P < 0.0001. Data are presented as mean ± SEM.

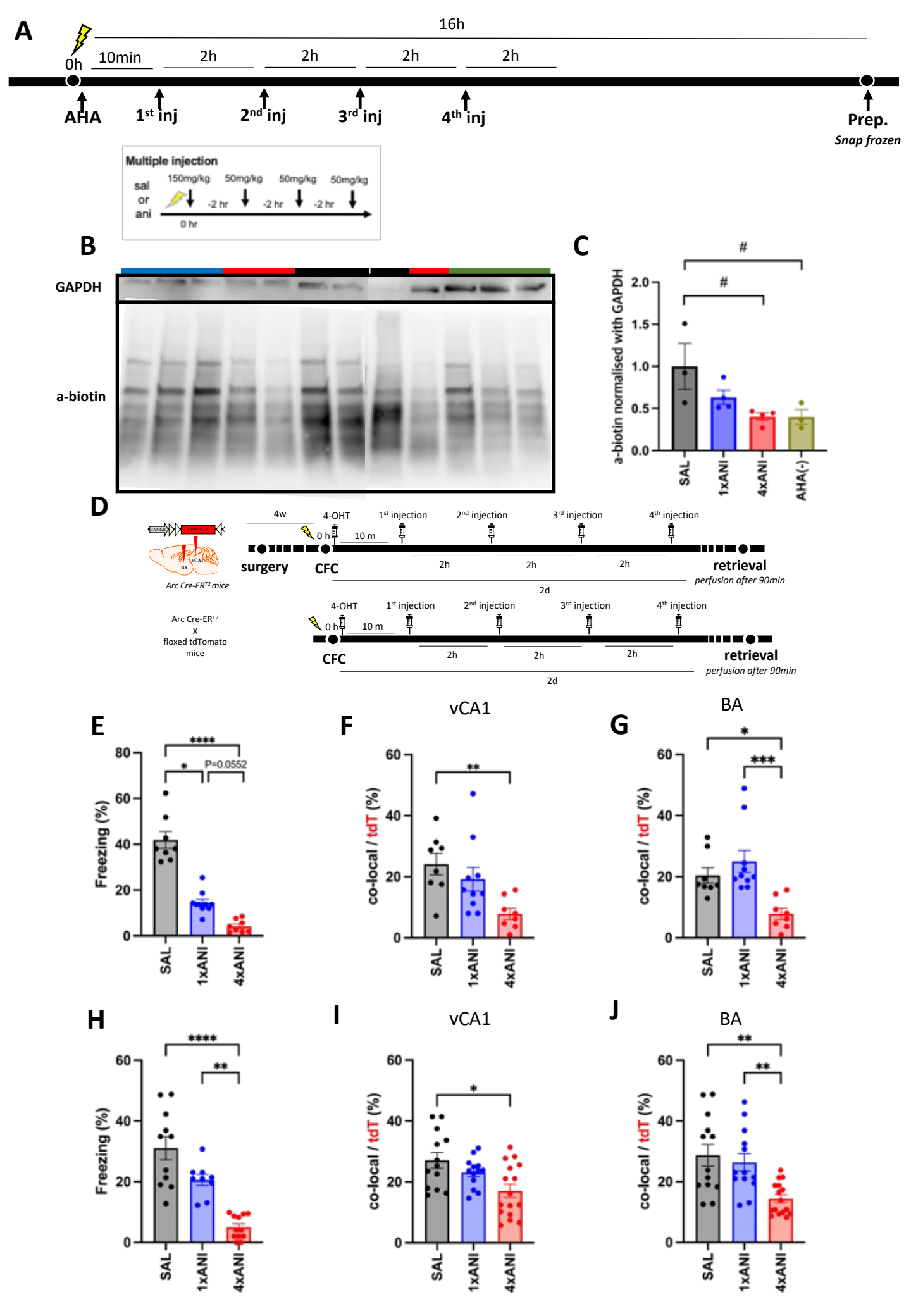
A
16h
0h
10min
2h
2h
2h
2h
AHA
1st inj
2nd inj
3rd inj
4th inj
Prep.
Snap frozen
Multiple injection
sal or ani
150mg/kg
50mg/kg
50mg/kg
50mg/kg
-2 hr
-2 hr
-2 hr
0 hr
B
GAPDH
a-biotin
C
a-biotin normalised with GAPDH
SAL
1xANI
4xANI
AHA(-)
D
4w
4-OHT
1st injection
2nd injection
3rd injection
4th injection
0 h
10 m
surgery
CFC
2h
retrieval
perfusion after 90min
2d
Arc Cre-ERT2 mice
Arc Cre-ERT2 X floxed tdTomato mice
E
Freezing (%)
P=0.0552
F
vCA1
co-local / tdT (%)
G
BA
H
I
J

Fig 2. Engram cells are less reactivated by fear recall with multiple anisomycin injections.

(A) Behavioural procedure for NCAA labelling.

(B) Western blot image to tag *de novo* synthesized proteins during memory acquisition

(C) Quantification of the de novo protein synthesis level normalised using GAPDH. SAL group, N = 3; 1xANI group, N = 4; 4xANI group, N = 4; AHA(-) group, N = 3. Kruskal-Wallis test followed by two-stage linear step-up procedure of Bejamini, Kriegar and Yekutieli. #P = 0.0776. Data are presented as mean ± SEM.

(D) Behavioural procedure for testing engram reactivation ratio.

(E-J) Data of engram reactivation analysis for Arc-CreERT2 mice expressing viral CaMKII-DIO-tdTomato (E-G) or crossed with floxed tdTomato (H-J). (E, H) Freezing level during memory recall session. 4xANI group showed lower freezing level compared to that of 1xANI group in both conditions. Engram reactivation ratio of vCA1 neurones (F, I) and BA neurones (G, J). Significantly lower reactivation ratio of BA neurones was observed in 4xANI group compared to 1xANI group. (E-G) SAL group, N = 8; 1xANI group, N = 10; 4xANI group, N = 8. (H-J) SAL group, N = 13; 1xANI group, N = 13; 4xANI group, N = 16. Kruskal-Wallis test followed by Dunn's multiple comparison test. (E) *P = 0.0336; ****P < 0.0001. (F) **P = 0.0045. (G) *P = 0.0148; ***P = 0.0003. (H) ****P < 0.0001; **P = 0.0033. (I) *P = 0.0230. (J) SAL vs. 4xANI, **P = 0.0027; 1xANI vs. 4xANI, **P = 0.0041. Data are presented as mean ± SEM.

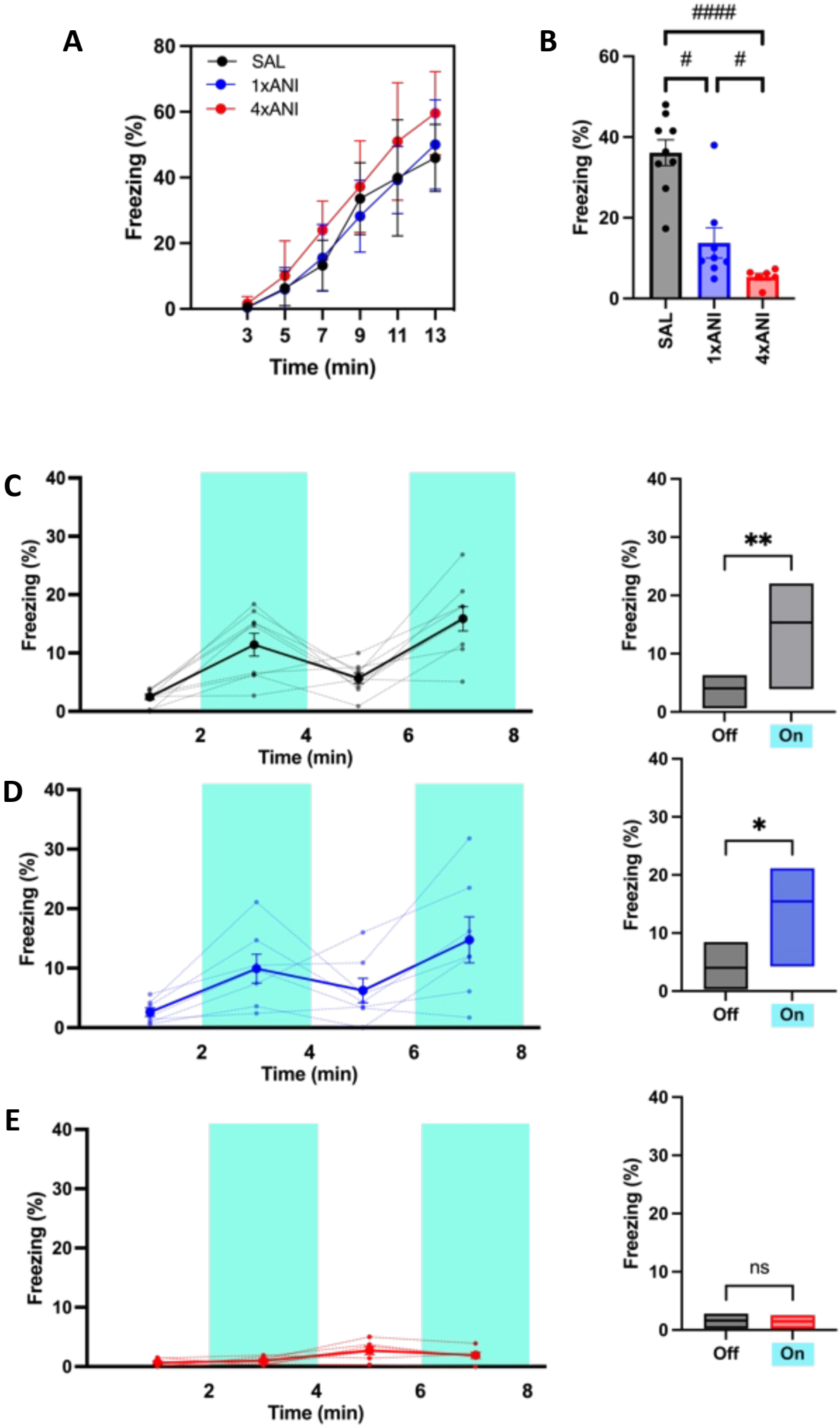
A
SAL
1xANI
4xANI
Freezing (%)
Time (min)
B
#####
#
#
Freezing (%)
SAL
1xANI
4xANI
C
Freezing (%)
Time (min)
**
Off
On
D
Freezing (%)
Time (min)
*
Off
On
E
Freezing (%)
Time (min)
ns
Off
On

Figure 3. Memory cannot be artificially recalled when protein synthesis was blocked for extensive time during memory acquisition.

(A) Freezing level during memory acquisition. Data are presented as mean ± SEM.

(B) Freezing level during contextual fear memory retrieval. SAL group, N = 9; 1xANI group, N = 7; 4xANI group, N = 6. Kruskal-Wallis test followed by two-stage linear step-up procedure of Bejamini, Kriegar and Yekutieli. SAL vs. 1xANI, $^{\#}q = 0.0193$; 1xANI vs. 4xANI, $^{\#}q = 0.0859$; $^{\#\#\#\#}q < 0.0001$. Data are presented as mean ± SEM.

(C-E) Optogenetic activation of vCA1 engram axon terminals in BA of mice treated with PSI during memory acquisition. Mice expressing ChR2 in vCA1 engram cells from CFC show greater freezing during light-on in saline treated control group (C) or by a single treatment of anisomycin (D) while absence of freezing behaviour was shown in mice treated with multiple injection of anisomycin (E). Wilcoxon test. SAL group, **P = 0.0078; 1xANI group, *P = 0.0156. Data are presented as mean ± SEM (left) or median (right).

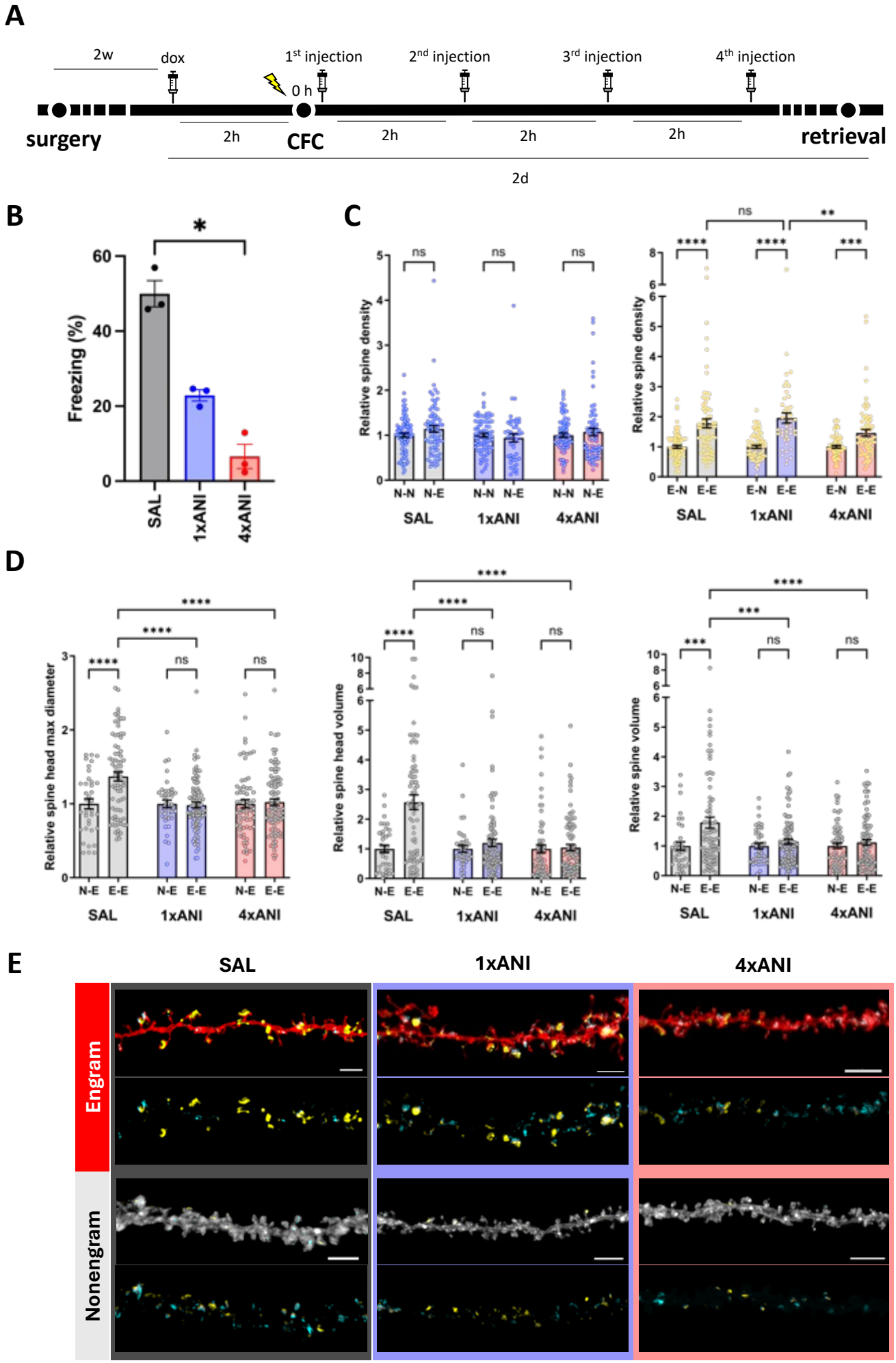
A
2w
dox
1st injection
2nd injection
3rd injection
4th injection
0 h
surgery
2h
CFC
2h
2h
2h
retrieval
2d
B
Freezing (%)
SAL
1xANI
4xANI
C
Relative spine density
N-N
N-E
E-N
E-E
ns
D
Relative spine head max diameter
Relative spine head volume
Relative spine volume
E
SAL
1xANI
4xANI
Engram
Nonengram

Figure 4. Reduced E-E Synapse Density using dual-eGRASP correlates with impaired optogenetic reactivation in 4xANI

(A) Schematic of the behavioural experiment. Mice were intraperitoneally injected with doxycycline 2 hours prior to CFC. After CFC, 4 consecutive anisomycin was intraperitoneally delivered. 2 days following CFC, mice were subjected to fear memory retrieval.

(B) Freezing level during contextual fear memory retrieval for the dual-eGRASP experiment. SAL group, N = 3; 1xANI group, N = 3; 4xANI group, N = 3. Kruskal-Wallis test followed by Dunn's multiple comparison test. *P = 0.0219. Data are presented as mean ± SEM.

(C) Normalised cyan/yellow eGRASP per dendritic length. The densities of cyan-only or yellow puncta on red dendrites are normalised to the corresponding cyan-only or yellow puncta on near-infrared dendrites from the same images to exclude the effect of different number of vCA1 cells expressing each presynaptic component. Each data point represents a dendrite. SAL group, n = 85 for BA nonengram dendrites, n = 74 for BA engram dendrites; 1xANI group, n = 70 for BA nonengram dendrites; n = 45 for BA engram dendrites; 4xANI group, n = 75 for BA nonengram dendrites; n = 69 for BA engram dendrites. Two-way ANOVA followed by Tukey's multiple comparison test. **P = 0.0043; ***P = 0.0008; ****P < 0.0001. Data are presented as mean ± SEM.

(D) Normalised spine head diameter, spine head volume and spine volume of dendrites from BA engram cells. SAL group N-E, n = 36; E-E, n = 76; 1xANI group N-E, n = 39; E-E, n = 93; 4xANI group N-E, n = 66; E-E, n = 93. Two-way ANOVA followed by Turkey's multiple comparison test. spine head diameter ****P < 0.0001, spine head volume ****P < 0.0001, spine volume ***P = 0.0001; ****P < 0.0001. Data are presented as mean ± SEM.

(E) Representative confocal image of both engram and nonengram dendrites from all three behavioural groups. Scale bar : SAL engram, 3 μm; SAL nonengram, 4 μm; 1xANI engram, 4 μm; 1xANI nonengram, 5 μm; 4xANI engram, 5 μm; 4xANI nonengram, 6 μm.

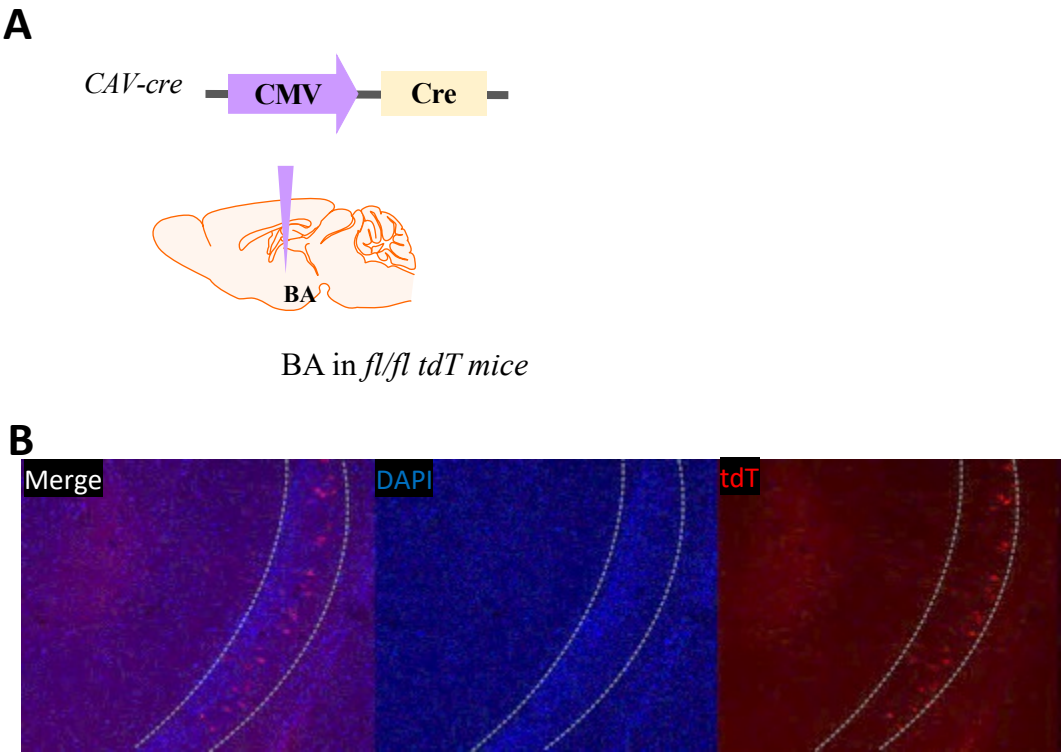

Fig. S1

vCA1 neurones projecting to the BA are mainly residing in the superficial layer

(A) CAV-Cre virus injected into the BA of double floxed tdTomato mice

(B) Images showing BA-projecting vCA1 neurones (tdT^+)

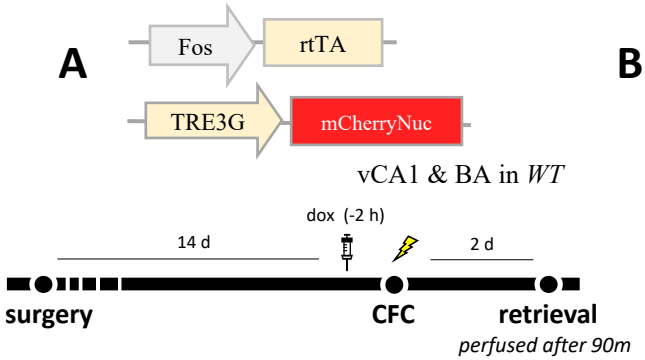
A
Fos
rtTA
TRE3G
mCherryNuc
vCA1 & BA in *WT*
dox (-2 h)
14 d
2 d
surgery
CFC
retrieval
perfused after 90m

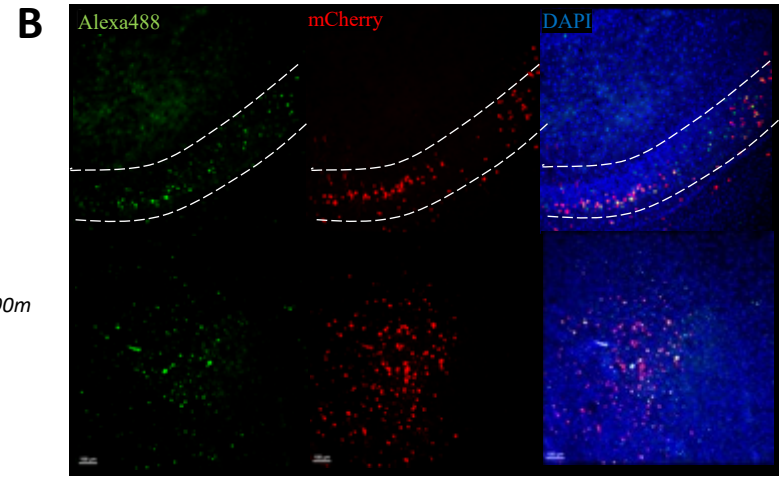
B
Alexa488
mCherry
DAPI

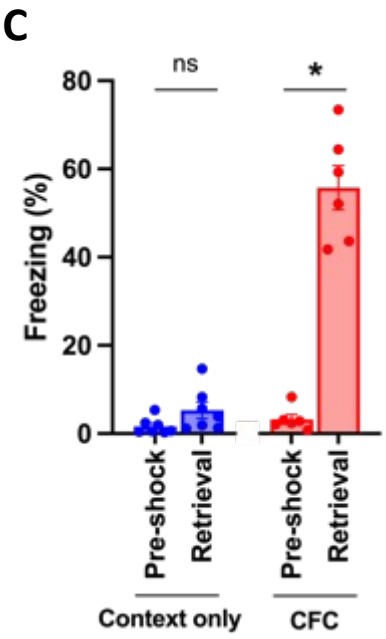
C
ns
*
Freezing (%)
80
60
40
20
0
Pre-shock
Retrieval
Pre-shock
Retrieval
Context only
CFC

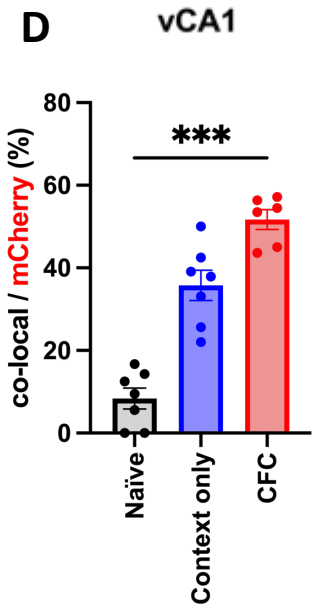
D
vCA1
***
co-local / mCherry (%)
80
60
40
20
0
Naïve
Context only
CFC

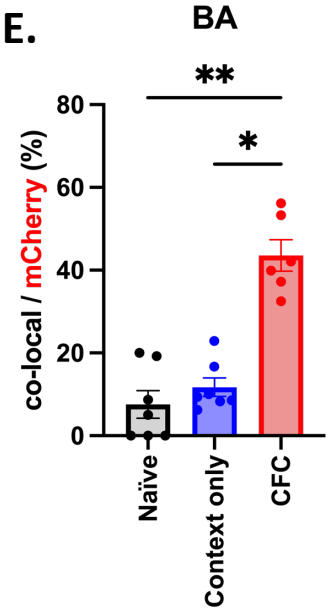
E.
BA
**
*
co-local / mCherry (%)
80
60
40
20
0
Naïve
Context only
CFC

Fig. S2

Fig S2. Engram reactivation of the vCA1 and BA during contextual fear conditioning.

(A) AAV1/2 containing Fos-rtTA/ TRE-mCherryNuc was injected into the vCA1 and BA of wild type mice.

(B) Representative image of the vCA1 (top) and BA (bottom). Neurons activated during the CFC were labelled in mCherry (middle) while neurons activated during memory retrieval were labelled in Alexa488 (left)

(C) Freezing level comparing between to pre-shock session and memory retrieval session. Context only group, N = 7; CFC group, N = 6. Wilcoxon test. *P = 0.0312. Data are presented as mean ± SEM.

(D-E) Reactivation ratio of engram cells in the vCA1 (**D**) and BA (**E**) in three groups: naïve, context only, and CFC. Naïve group, N = 7; context only group, N = 7; CFC group, N = 6. Wilcoxon test. ***P = 0.0002; **P = 0.0016; *P = 0.0256. Data are presented as mean ± SEM.

Fig. S3

A

	Pre-region	Post-region
	non engram	non engram
	engram	non engram
	non engram	engram
	engram	engram

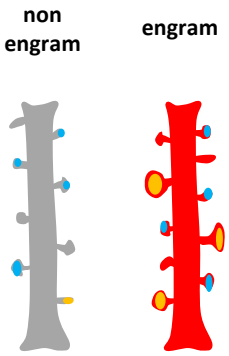

B

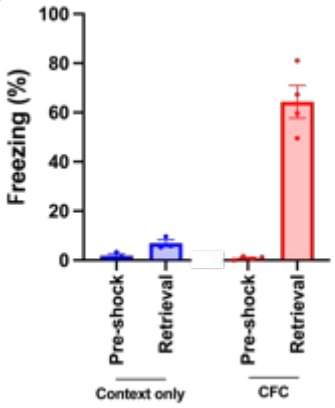

C

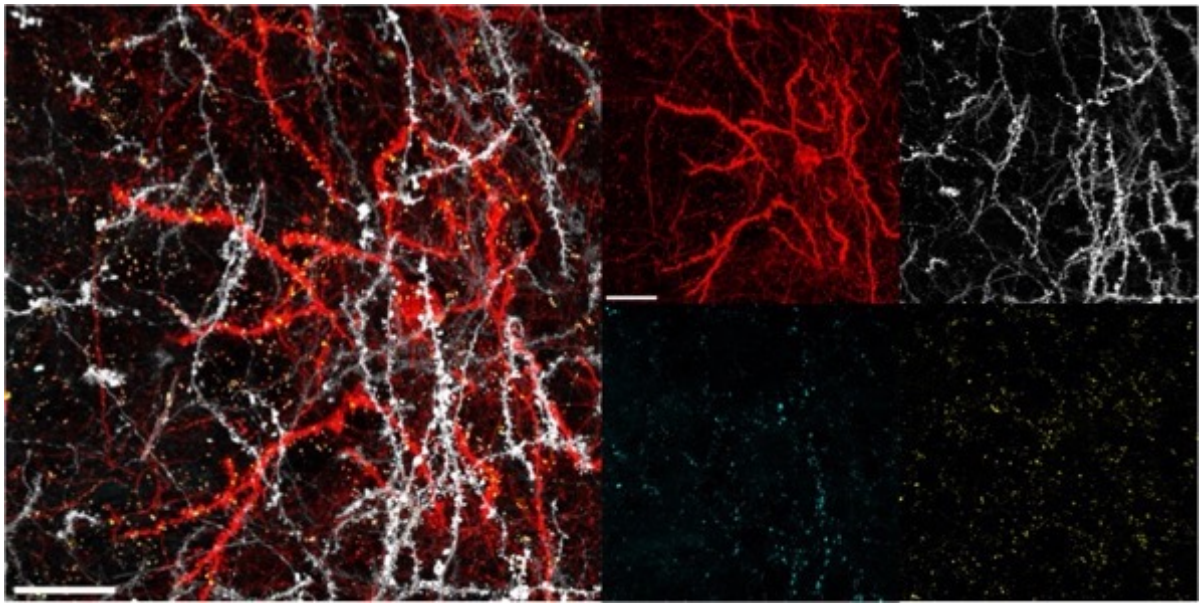

D

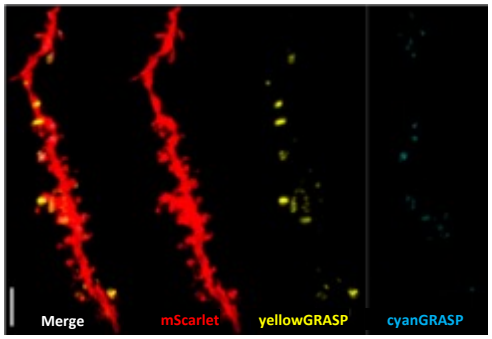

E

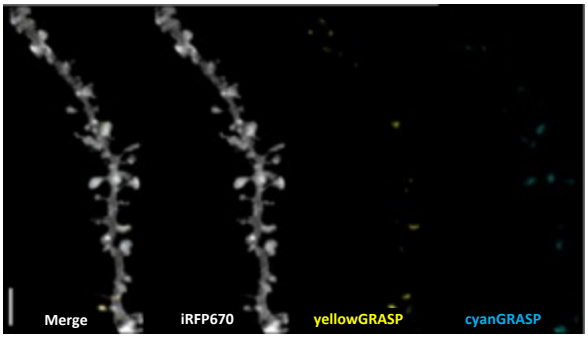

F

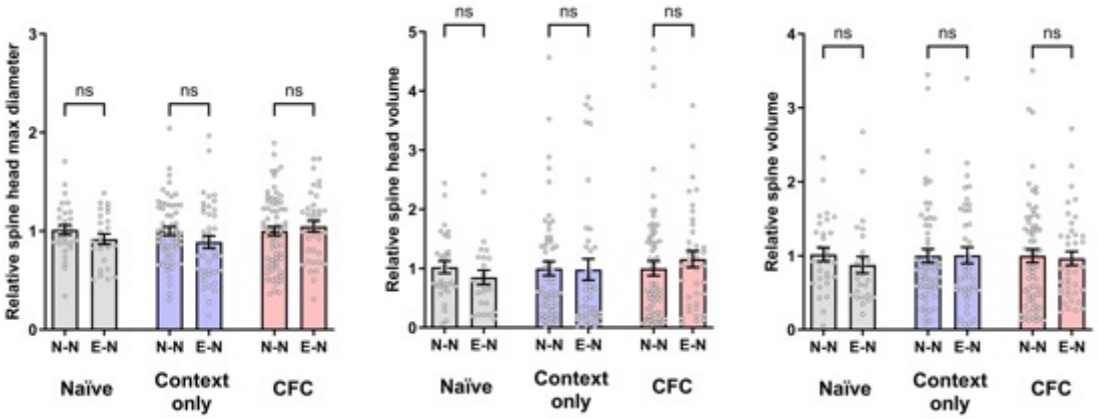

Fig S3.The overall synaptic connectivity from the vCA1 to the BA was not altered following the formation of memory.

(A) Categorisation of the four synaptic populations, represented by distinct colours.

(B) Freezing level during memory recall session for each group. Context only group, N = 3; CFC group, N = 4. Data are presented as mean ± SEM.

(C) Illustrative images depicting both engram (E) and nonengram (N) dendrites featuring GRASP signals in the BA. Scale bar : 30 μm

(D-E) Representative image of non-activated (D) and activated (E) GRASP signals displayed by each channel. Scale bar : 5 μm

(F) Normalised spine head diameters, spine head volume and spine volume of dendrites from BA non engram cells. Sizes of the spines with yellow puncta were normalised to those of the spines with cyan-only puncta of the same dendrite. Each data point represents a spine. Naïve group N-N, n = 30; E-N, n = 26; Context only group N-N, n = 57; E-N, n = 41; CFC group N-N, n = 66; E-N, n = 39. Two-way ANOVA followed by Tukey's multiple comparison test. Data are represented as mean ± SEM

Fig. S4

A

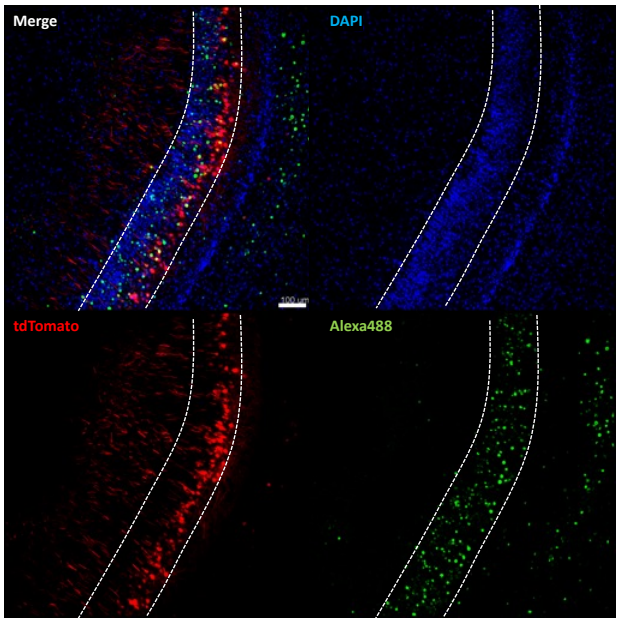

B

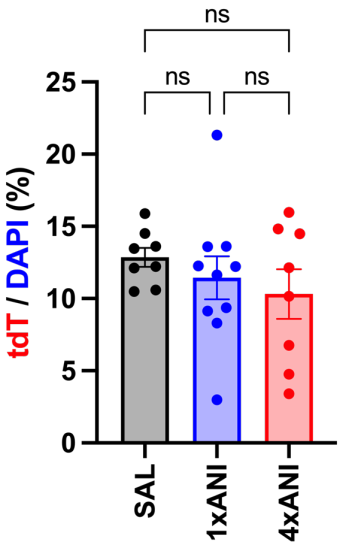

C

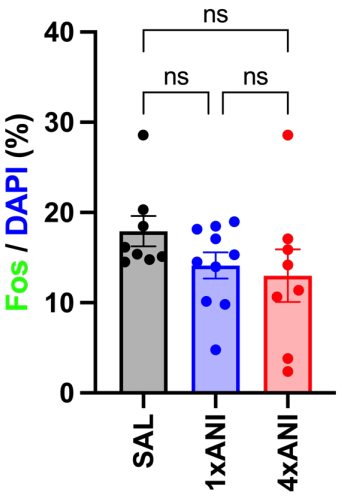

D

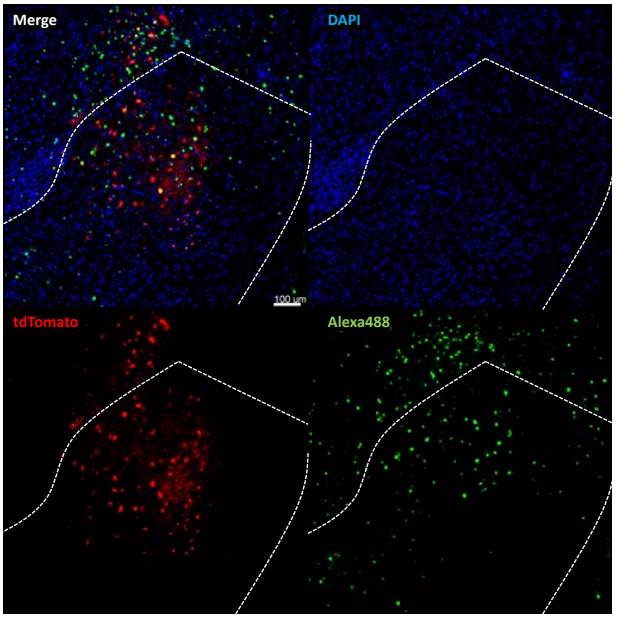

E

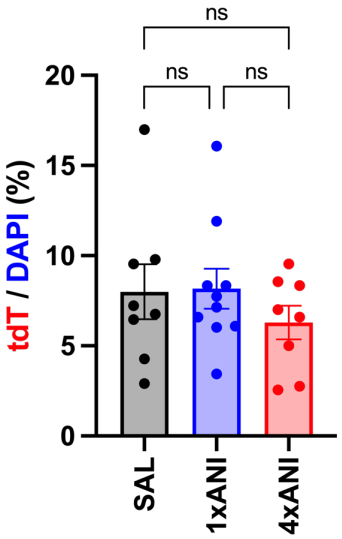

F

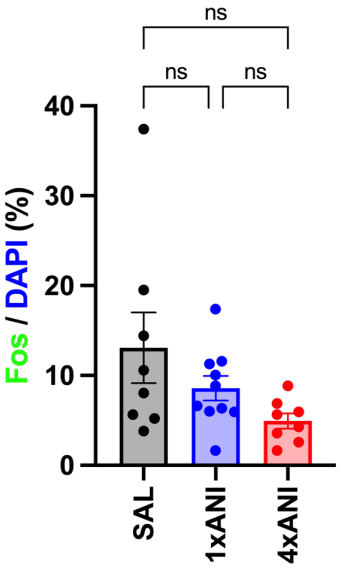

Fig S4. Engram labelling with PSI injections in Arc-TRAP mice.

(A) Representative images of activated neurones during the fear conditioning (tdTomato^{+}) in the vCA1 recall and neurones active during memory recall using cFos IHC (Alexa488). DAPI was stained to label the nuclei.

(B-C) cFos IHC result for the vCA1.

(D) Representative images of activated neurones during the fear conditioning (tdTomato^{+}) in the BA recall and neurones active during memory recall using cFos IHC (Alexa488). DAPI was stained to label the nuclei.

(D-E) cFos IHC result for the BA.

Fig. S5

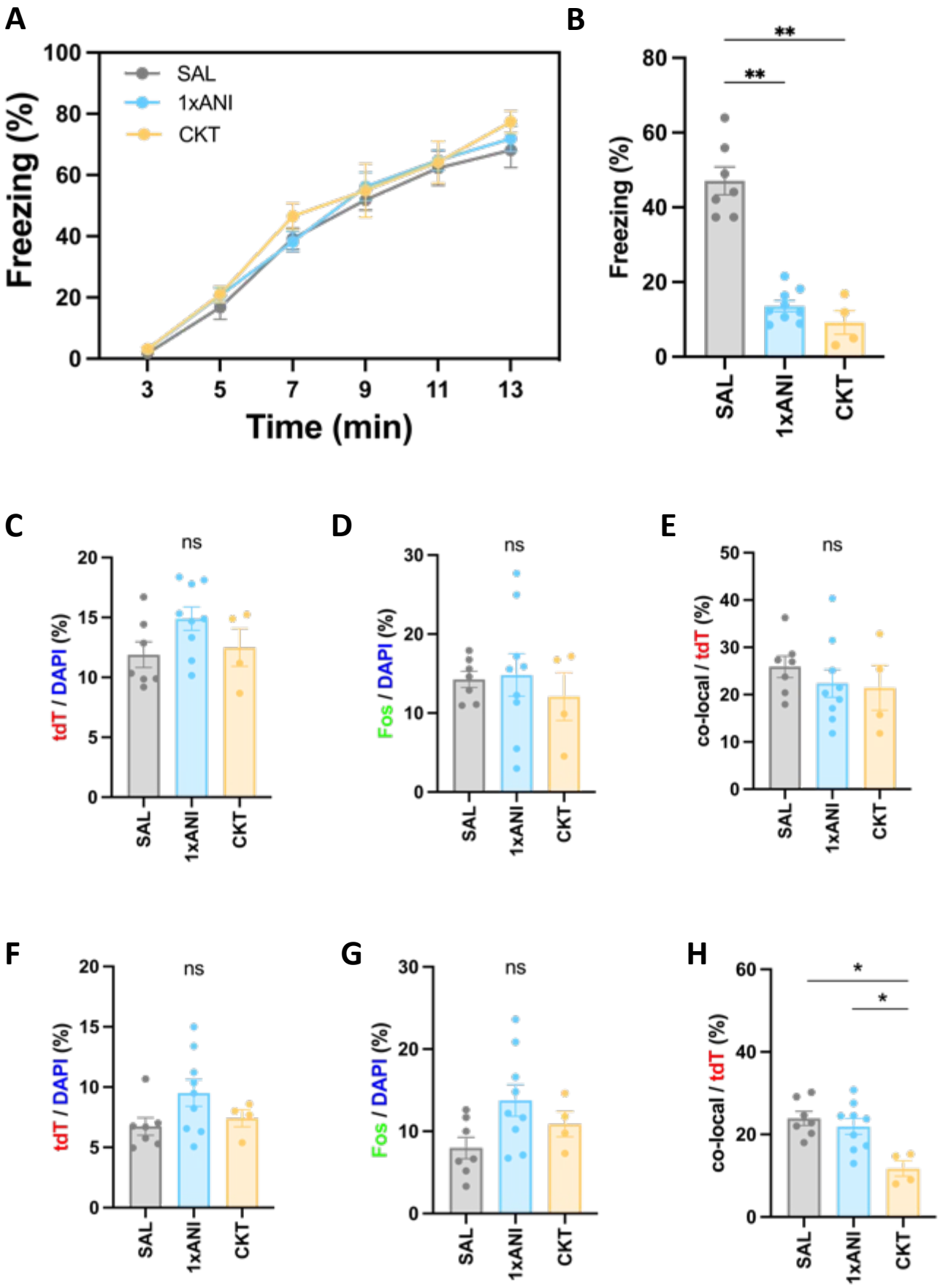
A
Freezing (%)
SAL
1xANI
CKT
Time (min)
B
Freezing (%)
**
**
SAL
1xANI
CKT
C
tdT / DAPI (%)
ns
D
Fos / DAPI (%)
ns
E
co-local / tdT (%)
ns
F
tdT / DAPI (%)
ns
G
Fos / DAPI (%)
ns
H
co-local / tdT (%)
*
*

Figure S5. Anisomycin combined with cycloheximide induced stronger retrograde amnesia.

(A) Acquisition plot for SAL, 1xANI, and CKT group during CFC. SAL group, N = 7; 1xANI group, N = 9; CKT group, N = 4. Data are presented as mean ± SEM.

(B) Freezing level during memory recall. Kruskal-Wallis test followed by Dunn's multiple comparison test. SAL vs. 1xANI, **P = 0.0067; SAL vs. CKT, **P = 0.0036. Data are presented as mean ± SEM.

(C-E) Immunohistochemistry data of vCA1. Kruskal-Wallis test followed by Dunn's multiple comparison test. Data are presented as mean ± SEM.

(F-H) Immunohistochemistry data of BA. Kruskal-Wallis test followed by Dunn's multiple comparison test. SAL vs. CKT, *P = 0.0148; 1xANI vs. CKT, *P = 0.0483. Data are presented as mean ± SEM.

Fig. S6

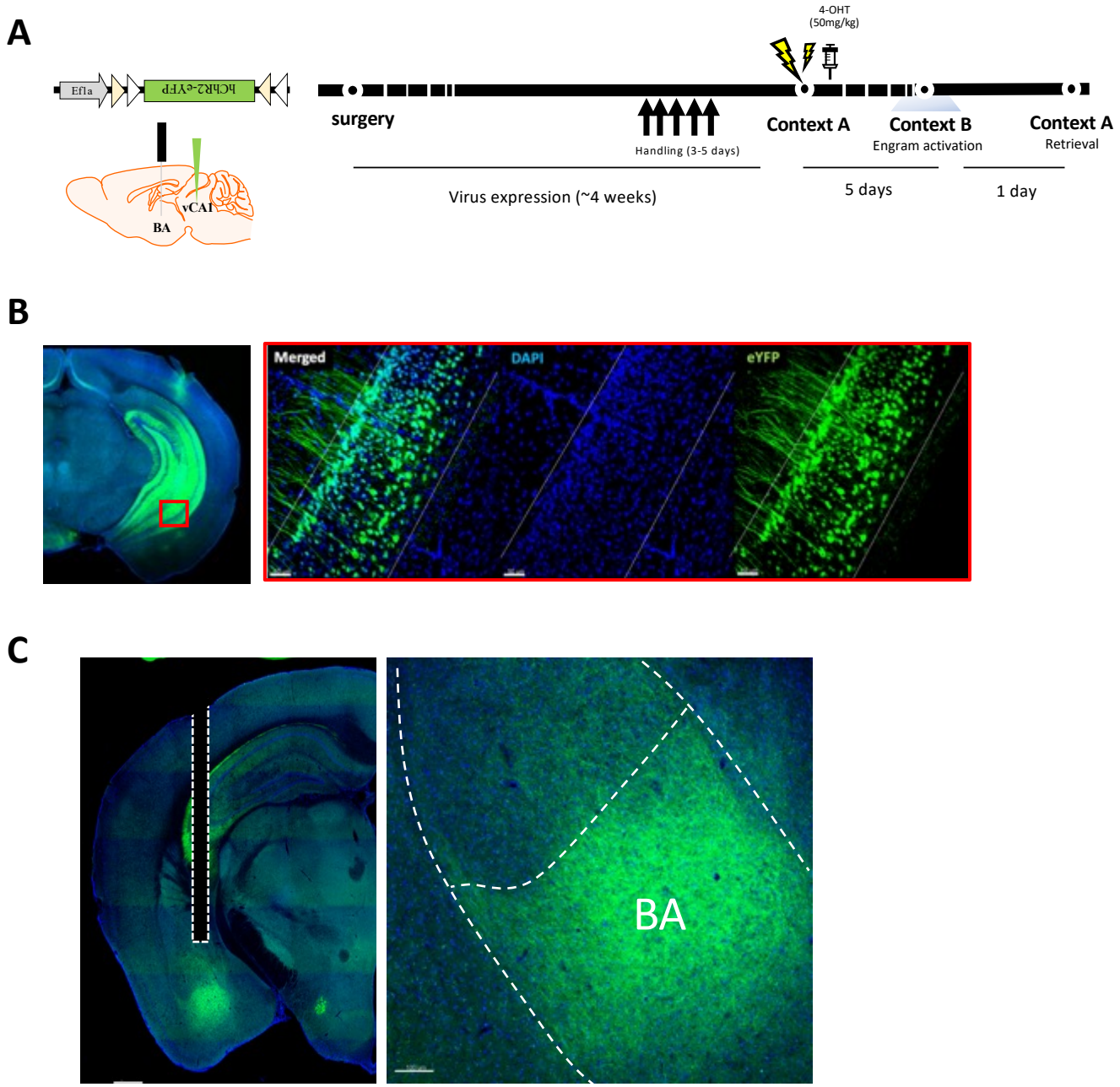

Fig S6. Representative images of virus expression for optogenetic behaviours. (**A**) Behavioural scheme (**B**) activated vCA1 neurones (**C**) vCA1 axonal projections to the BA expressed in ChR2-eYFP.

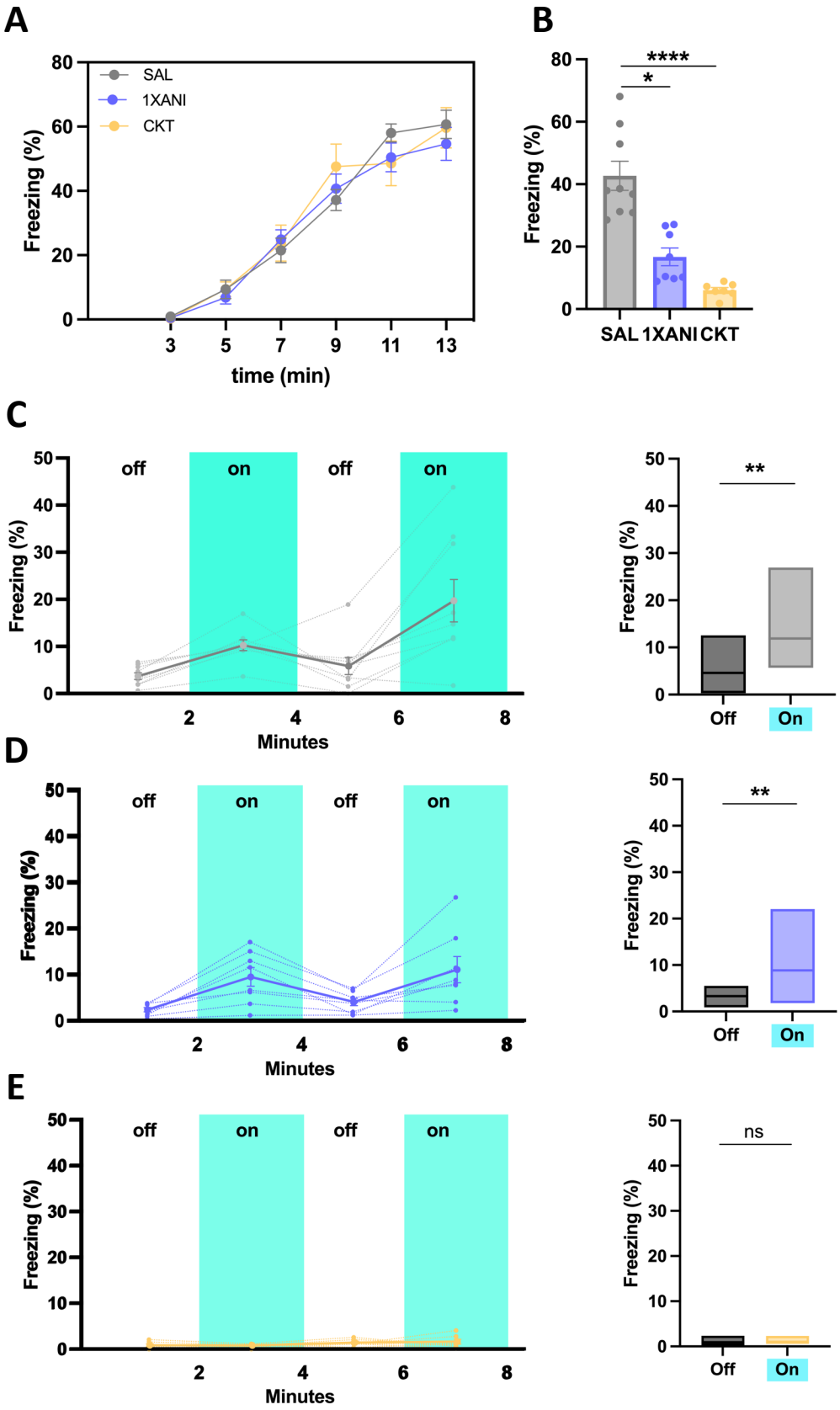
A
SAL
1XANI
CKT
Freezing (%)
time (min)
B
****
*
Freezing (%)
SAL
1XANI
CKT
C
off
on
off
on
Freezing (%)
Minutes
**
Off
On
D
off
on
off
on
Freezing (%)
Minutes
**
Off
On
E
off
on
off
on
Freezing (%)
Minutes
ns
Off
On

Fig S7. Memory cannot be artificially recalled when protein synthesis was blocked using combination of PSIs during memory acquisition.

(A) Freezing level during memory acquisition. Data are presented as mean ± SEM.

(B) Freezing level during contextual fear memory retrieval. SAL group, N = 9; 1xANI group, N = 8; CKT group, N = 7. Kruskal-Wallis test followed by Dunn's multiple comparison test. *P = 0.0380; ****P < 0.0003. Data are presented as mean ± SEM.

(C-E) Optogenetic activation of vCA1 engram axon terminals in BA of mice treated with different combination of PSI during memory acquisition. Mice expressing ChR2 in vCA1 engram cells show greater freezing during light-on epochs in saline-treated group (C) or by a single treatment of anisomycin (D) while absence of freezing behaviour was shown in mice treated with cocktail of PSI (E). Wilcoxon test. SAL group, **P = 0.0039; 1xANI group, **P = 0.0078. Data are presented as mean ± SEM (left) or median (right).

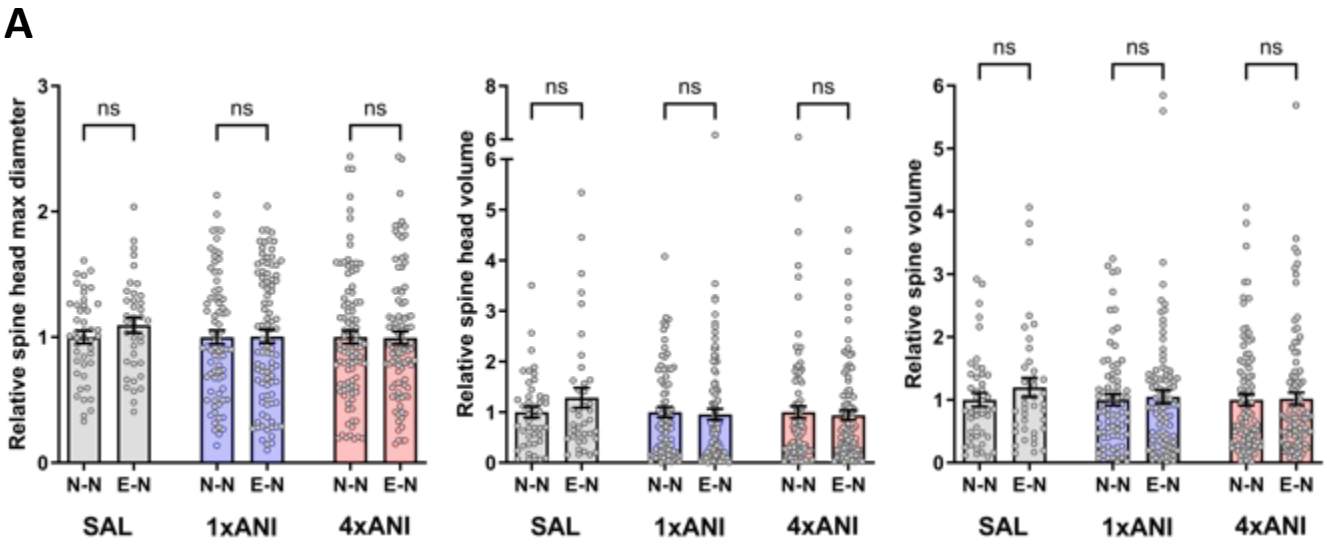

Fig S8. Normalised nonengram morphology after anisomycin treatment.

(A) Normalised spine head diameter, spine head volume and spine volume of dendrites from BA nonengram cells. SAL group N-N, $n = 44$; E-N, $n = 39$; 1xANI group N-N, $n = 77$; E-N, $n = 94$; 4xANI group N-N, $n = 96$; E-N, $n = 98$. Two-way ANOVA followed by Tukey's multiple comparison test. Data are presented as mean ± SEM.